The Journal of Chemical Physics

Signatures of light-induced nonadiabaticity in the field-dressed vibronic spectrum of formaldehyde

Cite as: J. Chem. Phys. **154**, 124308 (2021); https://doi.org/10.1063/5.0045069
Submitted: 22 January 2021 . Accepted: 07 March 2021 . Published Online: 24 March 2021

Csaba Fábri, Gábor J. Halász, Lorenz S. Cederbaum, and Ágnes Vibók

The Journal of Chemical Physics ARTICLE scitation.org/journal/jcp

Signatures of light-induced nonadiabaticity in the field-dressed vibronic spectrum of formaldehyde

Cite as: J. Chem. Phys. 154, 124308 (2021); doi: 10.1063/5.0045069
Submitted: 22 January 2021 • Accepted: 7 March 2021 •
Published Online: 24 March 2021

Csaba Fábri,[1,2,a)] Gábor J. Halász,[3] Lorenz S. Cederbaum,[4] and Ágnes Vibók[5,6,b)]

AFFILIATIONS

[1]Laboratory of Molecular Structure and Dynamics, Institute of Chemistry, Eötvös Loránd University, Pázmány Péter sétány 1/A, H-1117 Budapest, Hungary
[2]MTA-ELTE Complex Chemical Systems Research Group, P.O. Box 32, H-1518 Budapest 112, Hungary
[3]Department of Information Technology, University of Debrecen, P.O. Box 400, H-4002 Debrecen, Hungary
[4]Theoretische Chemie, Physikalisch-Chemisches Institut, Universität Heidelberg, Im Neuenheimer Feld 229, 69120 Heidelberg, Germany
[5]Department of Theoretical Physics, University of Debrecen, P.O. Box 400, H-4002 Debrecen, Hungary
[6]ELI-ALPS, ELI-HU Non-Profit Ltd., Dugonics tér 13, H-6720 Szeged, Hungary

Note: This paper is part of the JCP Special Collection in Honor of Women in Chemical Physics and Physical Chemistry.
[a)]**Electronic mail:** ficsaba@caesar.elte.hu
[b)]**Author to whom correspondence should be addressed:** vibok@phys.unideb.hu

ABSTRACT

Nonadiabatic coupling is absent between the electronic ground X and first excited (singlet) A states of formaldehyde. As laser fields can induce conical intersections between these two electronic states, formaldehyde is particularly suitable for investigating light-induced nonadiabaticity in a polyatomic molecule. The present work reports on the spectrum induced by light—the so-called field-dressed spectrum—probed by a weak laser pulse. A full-dimensional *ab initio* approach in the framework of Floquet-state representation is applied. The low-energy spectrum, which without the dressing field would correspond to an infrared vibrational spectrum in the X-state, and the high-energy spectrum, which without the dressing field would correspond to the X → A spectrum, are computed and analyzed. The spectra are shown to be highly sensitive to the frequency of the dressing light allowing one to isolate different nonadiabatic phenomena.

I. INTRODUCTION

It is widely accepted today that conical intersections (CIs), degeneracy points between multidimensional potential energy surfaces (PESs),[1–6] are of great importance in the case of polyatomic molecules. CIs play a fundamental role in nonadiabatic processes, which are ubiquitous in photophysics and photochemistry.[7–31] In several important photodynamical processes, such as molecular dissociation, fragmentation, isomerization, and so on, CIs can provide an efficient decay pathway for population transfer on the femtosecond timescale. Naturally occurring CIs, which are an inherent feature of polyatomic molecules, are called "natural CIs."

Exposing molecules to laser fields gives rise to CIs induced by light [light-induced conical intersection (LICI)], which cannot be avoided even in the case of diatomic molecules.[32,33] In diatomics, the angle between the molecular axis and the polarization vector of the external electric field becomes the missing dynamical variable that, together with the single vibrational coordinate, constitute the two-dimensional branching space in which the LICI exists. The energetic position of the LICI is determined by the laser frequency, and the strength of the nonadiabatic coupling is controlled by the light intensity. Similarly to the case of natural CIs, LICIs can give rise to a variety of nonadiabatic phenomena. Several theoretical and experimental studies have demonstrated, dominantly for diatomics,

that LICIs have remarkable effects on the different topological, spectroscopic, and dynamical properties of molecules.[34–43]

Studying light-induced nonadiabatic effects in polyatomic molecules is more challenging, and the outcome of such studies is expected to be richer than in diatomics. The existence of several vibrational degrees of freedom enables the definition of a branching space of the LICI without further involving any rotational coordinates. So far, few theoretical and experimental studies investigating light-induced nonadiabatic processes in polyatomics have become available.[44–46] This is mainly due to the fact that natural CIs are ubiquitous in polyatomics, and owing to the strong mixing between light-induced and natural nonadiabatic phenomena, their unequivocal distinction is rather challenging. Therefore, it is desirable at first to consider situations where a clear separation of effects caused by natural and light-induced CIs can be made, so as to identify the effects purely caused by the LICI.

In a recently published study,[47] a clear fingerprint of the LICI has been demonstrated in the field-dressed low-energy vibronic spectrum of the formaldehyde (H_2CO) molecule. By employing accurate full-dimensional quantum-dynamical calculations, the so-called intensity borrowing effect has been identified in the field-dressed spectrum of H_2CO. Intensity borrowing can be seen as a characteristic fingerprint of nonadiabatic effects, manifested by irregular variations of spectral peak intensities and the appearance of unexpected energy levels. The four-atomic H_2CO molecule seems to be a favorable candidate for our purpose as its electronic structure permits the unambiguous identification of light-induced nonadiabatic phenomena, clearly separated from "natural" nonadiabatic effects. Namely, H_2CO not only lacks any natural CIs in the vicinity of the Franck–Condon region but also does not possess any first-order nonadiabatic coupling between the ground and first singlet excited electronic states around its equilibrium geometry.[48–50]

In the present work, we focus on the analysis of both the low-energy and high-energy regions of the field-dressed vibronic spectrum of H_2CO calculated by an accurate full-dimensional quantum-dynamical method. We will discuss in detail how the different laser frequencies and field polarization directions influence the impact of the LICI on the field-dressed spectrum.

The article is structured as follows: In Sec. II, the theoretical background of the current study is described and a two-step protocol for the simulation of the weak-field absorption and stimulated emission spectra of field-dressed polyatomic molecules is discussed. Section III presents and discusses the numerical results, and Sec. IV summarizes the conclusions.

II. THEORY AND COMPUTATIONAL PROTOCOL

Let us start with describing the working Hamiltonian and the two-step protocol used to compute the field-dressed absorption spectrum of molecules. In what follows, the two singlet electronic states S_0 ($\tilde{X}\,^1A_1$) and S_1 ($\tilde{A}\,^1A_2$) of H_2CO will be taken into account. The corresponding potential energy surfaces (PESs) are denoted by V_X and V_A, respectively. We assume that the electronic states X and A are coupled by a linearly polarized periodic electric field $\mathbf{E}(t) = E_0\mathbf{e}\cos(\omega t)$, where E_0, $\mathbf{e}$, and ω denote the amplitude, polarization, and angular frequency of the dressing laser field, respectively. In the static Floquet-state representation,[51,52] the Hamiltonian matrix has the form

$$\hat{H} = \begin{bmatrix} \hat{H}_{-n_{\max}} & \hat{D} & 0 & 0 & 0 & 0 & 0 \\ \hat{D}^\dagger & \ddots & \vdots & \vdots & \vdots & \iddots & 0 \\ 0 & \cdots & \hat{H}_{-1} & \hat{D} & 0 & \cdots & 0 \\ 0 & \cdots & \hat{D}^\dagger & \hat{H}_0 & \hat{D} & \cdots & 0 \\ 0 & \cdots & 0 & \hat{D}^\dagger & \hat{H}_1 & \cdots & 0 \\ 0 & \iddots & \vdots & \vdots & \vdots & \ddots & \hat{D} \\ 0 & 0 & 0 & 0 & 0 & \hat{D}^\dagger & \hat{H}_{n_{\max}} \end{bmatrix} \tag{1}$$

with

$$\hat{H}_n = \begin{bmatrix} \hat{T} + V_X + n\hbar\omega & 0 \\ 0 & \hat{T} + V_A + n\hbar\omega \end{bmatrix} \tag{2}$$

and

$$\hat{D} = \begin{bmatrix} W_X & W \\ W & W_A \end{bmatrix}, \tag{3}$$

where $\hat{T}$ is the vibrational kinetic energy operator and $n = -n_{\max}, \ldots, n_{\max}$ is the Fourier index that labels the different light-induced potential channels. The operators $W = -\mathbf{d}(\mathbf{R})\mathbf{e}E_0/2$, $W_X = -\mathbf{d}_X(\mathbf{R})\mathbf{e}E_0/2$, and $W_A = -\mathbf{d}_A(\mathbf{R})\mathbf{e}E_0/2$ describe the interaction between the external electric field and the transition dipole moment [TDM, $\mathbf{d}(\mathbf{R})$] as well as the permanent dipole moments [PDMs, $\mathbf{d}_X(\mathbf{R})$ and $\mathbf{d}_A(\mathbf{R})$] of the electronic states X and A. The rotational degrees of freedom are omitted from the current computational protocol, and the orientation of the molecule is kept fixed with respect to the external electric field.

The field-dressed eigenfunctions $|\Phi_k\rangle$ and eigenvalues ϵ_k (called quasienergies) can be obtained by diagonalizing the Hamiltonian of Eq. (1). The eigenfunctions $|\Phi_k\rangle$ can be expanded as the linear combination of products of field-free molecular vibronic eigenstates (denoted by $|Xi\rangle$ and $|Ai\rangle$ for the electronic states X and A, respectively) and the Fourier vectors of the Floquet states, that is,

$$|\Phi_k\rangle = \sum_{\alpha=X,A} \sum_i \sum_n c_{\alpha i n}^{(k)} |\alpha i\rangle |n\rangle. \tag{4}$$

In Eq. (4), i labels vibrational eigenstates and $|n\rangle$ is the nth Fourier vector of the Floquet state. The expansion coefficients $c_{\alpha i n}^{(k)}$ can be obtained by determining the eigenvectors of the light-dressed Hamiltonian of Eq. (1) after constructing its matrix representation. Note that it is often a good approximation to treat the two-dimensional blocks,

$$\hat{H}(n) = \begin{bmatrix} \hat{T} + V_X + n\hbar\omega & W \\ W & \hat{T} + V_A + (n-1)\hbar\omega \end{bmatrix}, \tag{5}$$

of the Hamiltonian of Eq. (1) separately (rotating wave approximation[53–55]). As $\hat{H}(n)$ contains matrix elements of $\hat{H}$ [see Eq. (1)] that are on the main diagonal as well as on the first diagonal below and above the main diagonal, the terms W_X and W_A are necessarily

missing from Eq. (5). In the case of Eq. (5), field-dressed states [eigenstates of the noninteracting $\hat{H}(n)$ blocks] can be written as

$$|\Phi_k(n)\rangle = \sum_i c^{(k)}_{\mathrm{X}in}|\mathrm{X}i\rangle|n\rangle + \sum_i c^{(k)}_{\mathrm{A}i,n-1}|\mathrm{A}i\rangle|n-1\rangle. \tag{6}$$

The full Hamiltonian $\hat{H}$ of Eq. (1) is employed exclusively in the numerical calculation of the spectra discussed in Sec. III. The effective Hamiltonian of Eq. (5) has been employed as well and found to give accurate results. Hence, we use the latter for analyzing the numerical results obtained with Eq. (1).

Next, we briefly discuss the spectroscopy of field-dressed molecules.[56] A weak probe pulse is assumed, and the transition amplitudes between field-dressed states $|\Phi_k\rangle$ and $|\Phi_l\rangle$ are evaluated using first-order time-dependent perturbation theory. The transition amplitudes are the matrix elements of the electric dipole moment operator $\hat{\mu}_\alpha$ ($\alpha = x, y, z$) between two field-dressed states of Eq. (4),

$$\begin{aligned}\langle\Phi_k|\hat{\mu}_\alpha|\Phi_l\rangle = &\sum_i\sum_j\sum_n c^{(k)*}_{\mathrm{X}in}c^{(l)}_{\mathrm{X}jn}\langle\mathrm{X}i|\hat{\mu}_\alpha|\mathrm{X}j\rangle\\ &+\sum_i\sum_j\sum_n c^{(k)*}_{\mathrm{A}in}c^{(l)}_{\mathrm{A}jn}\langle\mathrm{A}i|\hat{\mu}_\alpha|\mathrm{A}j\rangle\\ &+\sum_i\sum_j\sum_n c^{(k)*}_{\mathrm{X}in}c^{(l)}_{\mathrm{A}jn}\langle\mathrm{X}i|\hat{\mu}_\alpha|\mathrm{A}j\rangle\\ &+\sum_i\sum_j\sum_n c^{(k)*}_{\mathrm{A}in}c^{(l)}_{\mathrm{X}jn}\langle\mathrm{A}i|\hat{\mu}_\alpha|\mathrm{X}j\rangle.\end{aligned} \tag{7}$$

One can notice that while the first and second terms in Eq. (7) are associated with the PDMs of the electronic states X and A, the third and fourth terms involve the TDM. The expression in Eq. (7) describes both the field-dressed absorption and stimulated emission processes. The peaks associated with absorption and stimulated emission can be distinguished by comparing the quasienergies of the initial and final field-dressed states. The intensity of transitions between field-dressed states can be obtained as

$$I_{kl} \propto \omega_{kl}\sum_{\alpha=x,y,z}|\langle\Phi_k|\hat{\mu}_\alpha|\Phi_l\rangle|^2, \tag{8}$$

where $\omega_{kl} = (\epsilon_l - \epsilon_k)/\hbar$ denotes the angular frequency of the transition.

The V_{X} (S_0 electronic state, X) and V_{A} (S_1 electronic state, A) PESs are taken from Refs. 57 and 58, respectively. The corresponding vertical and adiabatic excitation energies are equal to 28 954 and 28 138 cm^{-1}. H_2CO has an equilibrium structure of C_{2v} point-group symmetry in its electronic ground state (X), as shown in Fig. 1. The six normal modes of H_2CO are summarized in Fig. 1 and Table I. The excited electronic state (A) has a double-well structure along the out-of-plane (ν_4) mode, and the two equivalent nonplanar equilibrium structures (C_s point-group symmetry) are connected by a planar transition state structure (C_{2v} point-group symmetry). The symmetries of the X and A electronic states are A_1 and A_2 at the Franck–Condon point of C_{2v} symmetry. Group theoretical considerations suggest that both the first-order nonadiabatic coupling and the TDM vector vanish at C_{2v} geometries (such as the Franck–Condon point). When making displacements along the vibrational mode of B_1 or B_2 symmetry, the first-order nonadiabatic coupling is expected to remain small at the resulting geometries of C_s symmetry.

The six-dimensional vibrational Schrödinger equation was solved by the numerically exact and general rovibrational code

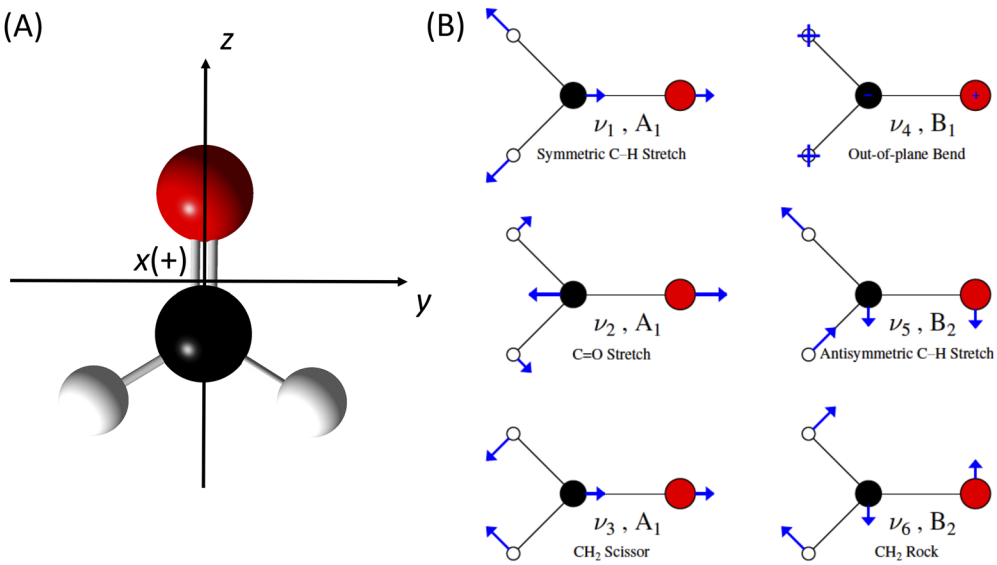

FIG. 1. Equilibrium structure [panel (a)] and normal modes [panel (b)] of H_2CO in its electronic ground state and definition of the body-fixed coordinate axes (the *x* axis is directed outwards, as indicated by the + sign).

TABLE I. Normal mode labels, C_{2v} irreducible representations (Γ), description of normal modes, and anharmonic fundamentals (ω, obtained by 6D variational computations in the electronic ground state of H_2CO, in units of cm^{-1}).

Label	Γ	Description	ω / cm^{-1}
ν_1	A_1	Sym C−H stretch	2728.4
ν_2	A_1	C=O stretch	1738.1
ν_3	A_1	CH_2 scissor	1466.0
ν_4	B_1	Out-of-plane bend	1147.0
ν_5	B_2	Antisym C−H stretch	2819.9
ν_6	B_2	CH_2 rock	1234.5

GENIUSH[59–61] for both electronic states. The vibrational computations employed polyspherical coordinates,[62] and the axes of the body-fixed frame were oriented according to the translational and rotational Eckart conditions[63] using the equilibrium structure of the X electronic state as the reference structure. The vibrational eigenstates were represented in a six-dimensional direct-product discrete variable representation basis, and atomic mass values m_C = 12.0 u, m_O = 15.994 915 u, and m_H = 1.007825 u were used throughout the nuclear motion computations. The vibrational Hamiltonian matrix was separated into four noninteracting blocks that correspond to the four irreducible representations of the S_2^* molecular symmetry group,[64] which is isomorphic to the C_{2v} point group. In order to facilitate the interpretation of our results, vibrational eigenstates of both electronic states were recalculated using rectilinear normal coordinates (corresponding to the X equilibrium structure for the electronic state X and to the A planar transition state structure for the electronic state A) by the DEWE program package.[65,66] One-dimensional wave function cuts along the normal coordinates were then evaluated, and the nodal structures of the one-dimensional wave function cuts were inspected to assign the vibrational eigenstates with harmonic oscillator quantum numbers.

The six-dimensional permanent and transition dipole moment, i.e., PDM and TDM, surfaces of H_2CO were represented by a second-order Taylor expansion using the polyspherical coordinates employed by the vibrational eigenstate computations. The Taylor series were centered either at the equilibrium structure of the X electronic state (TDM and X-state PDM) or at the transition state structure of the A electronic state (A-state PDM). The PDM and TDM vectors are referenced in the Eckart body-fixed frame described above, and the dipole derivatives needed by the Taylor expansion were evaluated numerically at the CAM-B3LYP/6-31G* level of theory by the finite-difference method. The symmetry properties of the body-fixed PDM and TDM components are provided in Table II.

TABLE II. Symmetry properties (C_{2v} irreducible representations, Γ) of the body-fixed components of the permanent (PDM) and transition (TDM) dipole moments.

Component	Γ_{PDM}	Γ_{TDM}
x	B_1	B_2
y	B_2	B_1
z	A_1	A_2

The quasienergies and field-dressed states were computed by diagonalizing the light-dressed Hamiltonian of Eq. (1) in the direct-product basis of field-free molecular eigenstates and Fourier vectors of the Floquet states $|n\rangle$. The maximal Fourier component was set to n_{max} = 2, which proved sufficient for obtaining converged numerical results.

III. RESULTS AND DISCUSSION

Having discussed the underlying theory and described the molecular system under investigation, we proceed to the analysis of light-induced nonadiabatic effects in the field-dressed spectrum of H_2CO. In all cases presented, the dressing field is assumed to be switched on adiabatically and the initial field-dressed state $|\Phi_i\rangle$ is chosen as the field-dressed state giving maximal overlap with the vibrational ground state of the X electronic state. In what follows, both the low-energy and high-energy spectral regions, corresponding to vibrational (no change in the electronic state) and vibronic (from the electronic state X to A) transitions, will be examined. Peak splitting effects (Sec. III A) analogous to the Autler–Townes effect[67] will be distinguished from intensity borrowing effects (Sec. III B). The analysis of the numerical results is facilitated by a theoretical model, which is based on Eqs. (5) and (6) and can be applied to both the peak splitting and intensity borrowing situations. The dressing parameters have been chosen in such a way that either some of the final field-dressed states (Sec. III A) or the initial field-dressed state (Sec. III B) is a superposition of two or more field-free eigenstates.

A. Peak splitting effects in the field-dressed spectrum

Figure 2 presents the field-free and field-dressed spectra of H_2CO; in the field-dressed case, the dressing wavenumber and intensity values are set to ω_d = 25 575.0 cm^{-1} and $I_d = 10^{11}$ W/cm^2, respectively. Both the low-energy and high-energy regions of the spectrum are displayed in Fig. 2. The dressing field is assumed to be linearly polarized, and we choose the polarization vectors $\mathbf{e}_x = (1, 0, 0)$, $\mathbf{e}_y = (0, 1, 0)$, and $\mathbf{e}_{xy} = (1, 1, 0)/\sqrt{2}$, all of which are referenced in the body-fixed frame.

First, we discuss the low-energy region of the spectrum that, in the absence of dressing, would consist of transitions from the X vibrational ground state to other X vibrational states. As we will see, the chosen dressing wavenumber in Fig. 2 is such that the field-free eigenstates at lower energies are hardly mixed by the dressing field; therefore, the low-energy field-dressed spectrum is very similar to the field-free spectrum.

With the dressing parameters of Fig. 2, the initial field-dressed state can be well approximated as

$$|\Phi_i(n)\rangle = |X0\rangle|n\rangle, \tag{9}$$

where $|X0\rangle$ denotes the vibrational ground state of the X electronic state. Moreover, the final field-dressed states

$$|\Phi_f(n)\rangle = |Xf\rangle|n\rangle \tag{10}$$

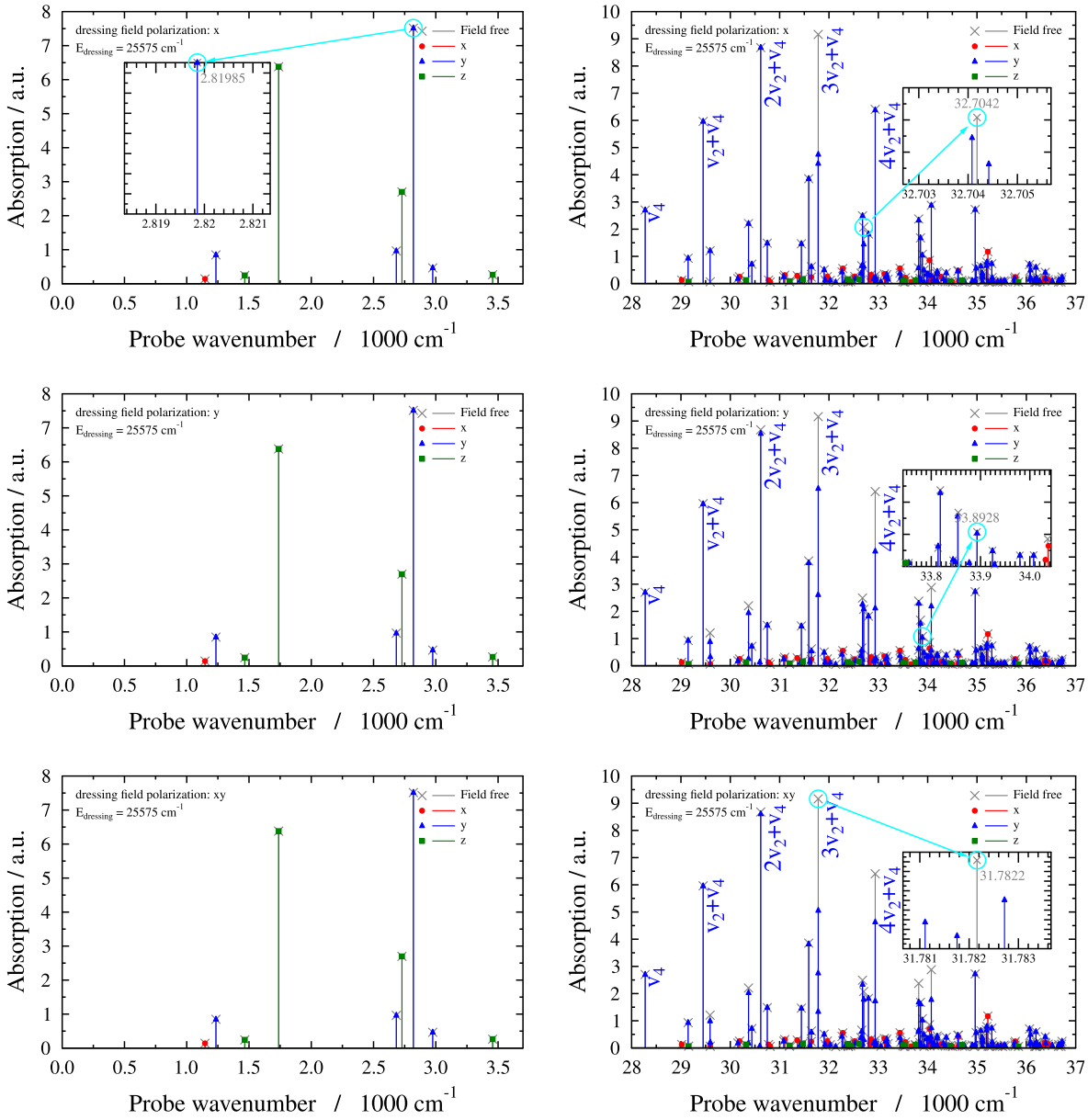

FIG. 2. Field-dressed and field-free spectra of the H_2CO molecule in the low-energy and high-energy regions. The dressing wavenumber and intensity equal ω_d = 25 575.0 cm^{-1} and $I_d = 10^{11}$ W/cm^2. The different polarization vectors [$\mathbf{e}_x$ = (1, 0, 0), $\mathbf{e}_y$ = (0, 1, 0), and $\mathbf{e}_{xy} = (1, 1, 0)/\sqrt{2}$] are given in the figure. Field-dressed transitions polarized along the *x*, *y*, and *z* axes are shown by the markers ●, ▲, and ■, respectively, while field-free transitions are indicated by the marker ×. Peaks of the high-energy field-free spectrum in the ν_4 (out-of-plane bend) progression with different numbers of quanta in the ν_2 (C=O stretch) vibrational mode are labeled with $v\nu_2 + \nu_4$ (v = 0, . . ., 4). At the chosen dressing wavenumber, the low-lying field-free states are hardly mixed by the dressing field; therefore, the low-energy field-free and field-dressed spectra look identical. At higher energies, mixings of field-free states occur (as the density of states grows) and peak splittings, highly sensitive to the polarization of the dressing field, appear in the field-dressed spectrum.

in the low-energy region also remain the eigenstates of the field-free molecule to a good approximation for all dressing polarizations considered. Therefore, the transition amplitudes between the dressed states $|\Phi_i(n)\rangle$ and $|\Phi_f(n)\rangle$ evaluate to

$$\langle\Phi_i(n)|\hat{\mu}_\alpha|\Phi_f(n)\rangle = \langle X0|\hat{\mu}_\alpha|Xf\rangle. \quad (11)$$

Eq. (11) implies that, for ω_d = 25 575.0 cm^{-1}, the field-free and field-dressed spectra are identical in the low-energy region, as can be seen

in Fig. 2. In other words, no new peaks or splittings of peaks appear in the low-energy part of the field-dressed spectrum. This finding is also supported by the inset in the upper left panel of Fig. 2 showing a selected peak of the low-energy spectral region.

The high-energy region of the field-free spectrum contains several peaks corresponding to transitions from the X vibrational ground state to A vibrational states. A striking feature of the high-energy region is the ν_4 progression, the corresponding transitions are labeled with the quantum numbers $v\nu_2 + \nu_4$ of the final A vibrational states in Fig. 2. The high-energy part of the field-dressed spectrum shows splittings of certain peaks of the field-free spectrum. Some of these splittings are featured by the insets in the right panels of Fig. 2. It is apparent in Fig. 2 that the field-dressed spectrum is sensitive to the choice of the polarization vector of the dressing field. In this case, higher-lying vibrational states are involved in the dressing process, which gives rise to mixings of field-free X and A vibrational levels due to the higher density of states. The mechanism of the peak splittings and the polarization dependence of the field-dressed spectrum can be understood by considering m field-dressed states of the form

$$|\Phi_{f'}(n+1)\rangle = \sum_{\beta=1}^{m-1} c^{(f')}_{\mathrm{X}k_\beta,n+1}|\mathrm{X}k_\beta\rangle|n+1\rangle + c^{(f')}_{\mathrm{A}jn}|\mathrm{A}j\rangle|n\rangle, \quad (12)$$

which are superpositions of $m-1$ X vibrational states and a single A vibrational eigenstate. The transition amplitude for the transitions $|\Phi_i(n)\rangle \rightarrow |\Phi_{f'}(n+1)\rangle$ reads

$$\langle\Phi_i(n)|\hat{\mu}_\alpha|\Phi_{f'}(n+1)\rangle = c^{(f')}_{\mathrm{A}jn}\langle\mathrm{X0}|\hat{\mu}_\alpha|\mathrm{A}j\rangle, \quad (13)$$

which implies that in the field-dressed case the system can make transitions from $|\Phi_i(n)\rangle$ to m $|\Phi_{f'}(n+1)\rangle$ states and the field-free peak $|\mathrm{X0}\rangle \rightarrow |\mathrm{A}j\rangle$ splits into m peaks in the field-dressed spectrum. It is important to note that since the coefficients $c^{(f')}_{\mathrm{X}k_\beta,n+1}$ and $c^{(f')}_{\mathrm{A}jn}$ are elements of an orthogonal transformation matrix, the sum of field-dressed transition probabilities over the manifold of the m $|\Phi_{f'}(n+1)\rangle$ states equals the transition probability of the field-free transition $|\mathrm{X0}\rangle \rightarrow |\mathrm{A}j\rangle$, that is,

$$\sum_{f'=1}^{m} |\langle\Phi_i(n)|\hat{\mu}_\alpha|\Phi_{f'}(n+1)\rangle|^2 = |\langle\mathrm{X0}|\hat{\mu}_\alpha|\mathrm{A}j\rangle|^2. \quad (14)$$

Equation (14) suggests that the intensity of the field-free transition $|\mathrm{X0}\rangle \rightarrow |\mathrm{A}j\rangle$ is distributed over the m different field-dressed transitions $|\Phi_i(n)\rangle \rightarrow |\Phi_{f'}(n+1)\rangle$.

The dressing wavenumber of $\omega_\mathrm{d} = 25\,575.0\ \mathrm{cm}^{-1}$ is nearly resonant with the vibronic transitions $|\mathrm{X}, \nu_3 + 2\nu_4 + 2\nu_6\rangle$ (6206.5 cm^{-1}, A_1 symmetry) $\rightarrow |\mathrm{A}, 3\nu_2 + \nu_4\rangle$ (31 782.2 cm^{-1}, B_1), $|\mathrm{X}, 3\nu_4 + \nu_5\rangle$ (6207.1 cm^{-1}, A_2) $\rightarrow |\mathrm{A}, 3\nu_2 + \nu_4\rangle$ (31 782.2 cm^{-1}, B_1), and $|\mathrm{X}, 2\nu_2 + \nu_3 + 2\nu_6\rangle$ (7362.3 cm^{-1}, A_1) $\rightarrow |\mathrm{A}, 4\nu_2 + \nu_4\rangle$ (32 937.2 cm^{-1}, B_1), leading to the formation of field-dressed states of Eq. (12). As the vibrational state $|\mathrm{A}, 3\nu_2 + \nu_4\rangle$ is coupled to $|\mathrm{X}, \nu_3 + 2\nu_4 + 2\nu_6\rangle$ by the y TDM component (B_1) and to $|\mathrm{X}, 3\nu_4 + \nu_5\rangle$ by the x TDM component (B_2), depending on the polarization of the dressing field, the field-free peak $3\nu_2 + \nu_4$ splits into three ($\mathbf{e} = \mathbf{e}_{xy}$) or two peaks ($\mathbf{e} = \mathbf{e}_y$ or $\mathbf{e} = \mathbf{e}_x$) in the field-dressed spectrum. In addition, the vibrational states $|\mathrm{A}, 4\nu_2 + \nu_4\rangle$ and $|\mathrm{X}, 2\nu_2 + \nu_3 + 2\nu_6\rangle$ are coupled by the y component of the TDM. Consequently, the field-free peak $4\nu_2 + \nu_4$ splits into two peaks in the field-dressed case if $\mathbf{e} = \mathbf{e}_{xy}$ or $\mathbf{e} = \mathbf{e}_y$ and no splitting occurs for $\mathbf{e} = \mathbf{e}_x$.

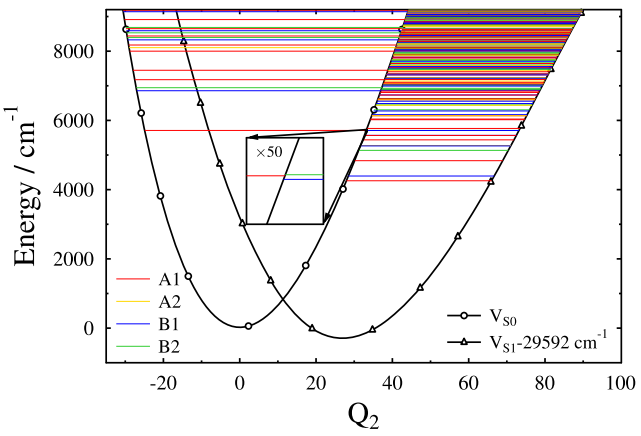

FIG. 3. One-dimensional field-free potential energy cuts (V_{S0} and V_{S1}) along the ν_2 (C=O stretch) normal mode (Q_2 denotes the normal coordinate of the ν_2 mode). The excited-state potential curve (V_{S1}) is shifted down by the photon energy value corresponding to the dressing wavenumber of 29 592.0 cm^{-1}. The vibrational energy levels are indicated by the horizontal lines with colors encoding irreducible representations of the C_{2v} point group.

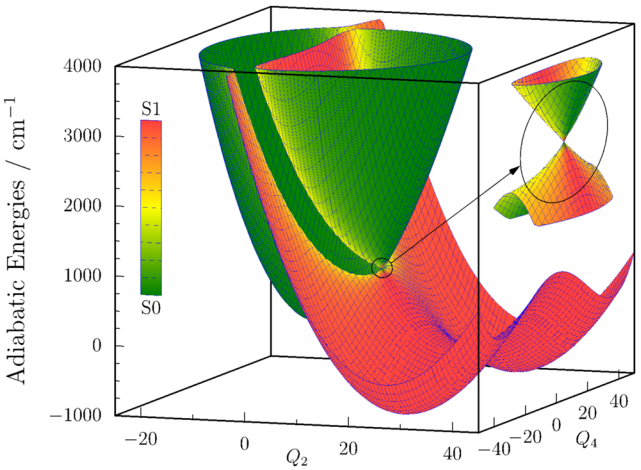

FIG. 4. Two-dimensional light-induced adiabatic potential energy surfaces along the ν_2 (C=O stretch) and ν_4 (out-of-plane bend) normal modes (Q_2 and Q_4 denote the normal coordinates of the modes ν_2 and ν_4). The dressing wavenumber and intensity are chosen as $\omega_\mathrm{d} = 29\,592.0\ \mathrm{cm}^{-1}$ and $I_\mathrm{d} = 10^{14}\ \mathrm{W/cm}^2$, respectively, and the dressing field is polarized along the body-fixed y axis. Note that this dressing intensity value is chosen for a better visualization only. The light-induced conical intersection is highlighted in the inset on the right-hand side. The character of the light-induced adiabatic potential energy surfaces is indicated by different colors (see the legend on the left).

B. Intensity borrowing effects in the field-dressed spectrum

If the dressing field couples the X vibrational ground state to m A vibrational states, the initial field-dressed state becomes

$$|\Phi_i(n)\rangle = c^{(i)}_{\mathrm{X}0n}|\mathrm{X}0\rangle|n\rangle + \sum_{\beta=1}^{m} c^{(i)}_{\mathrm{A}k_\beta,n-1}|\mathrm{A}k_\beta\rangle|n-1\rangle. \quad (15)$$

Such a situation is featured in Fig. 3 where one-dimensional cuts of the ground-state and excited-state PESs are shown along the ν_2

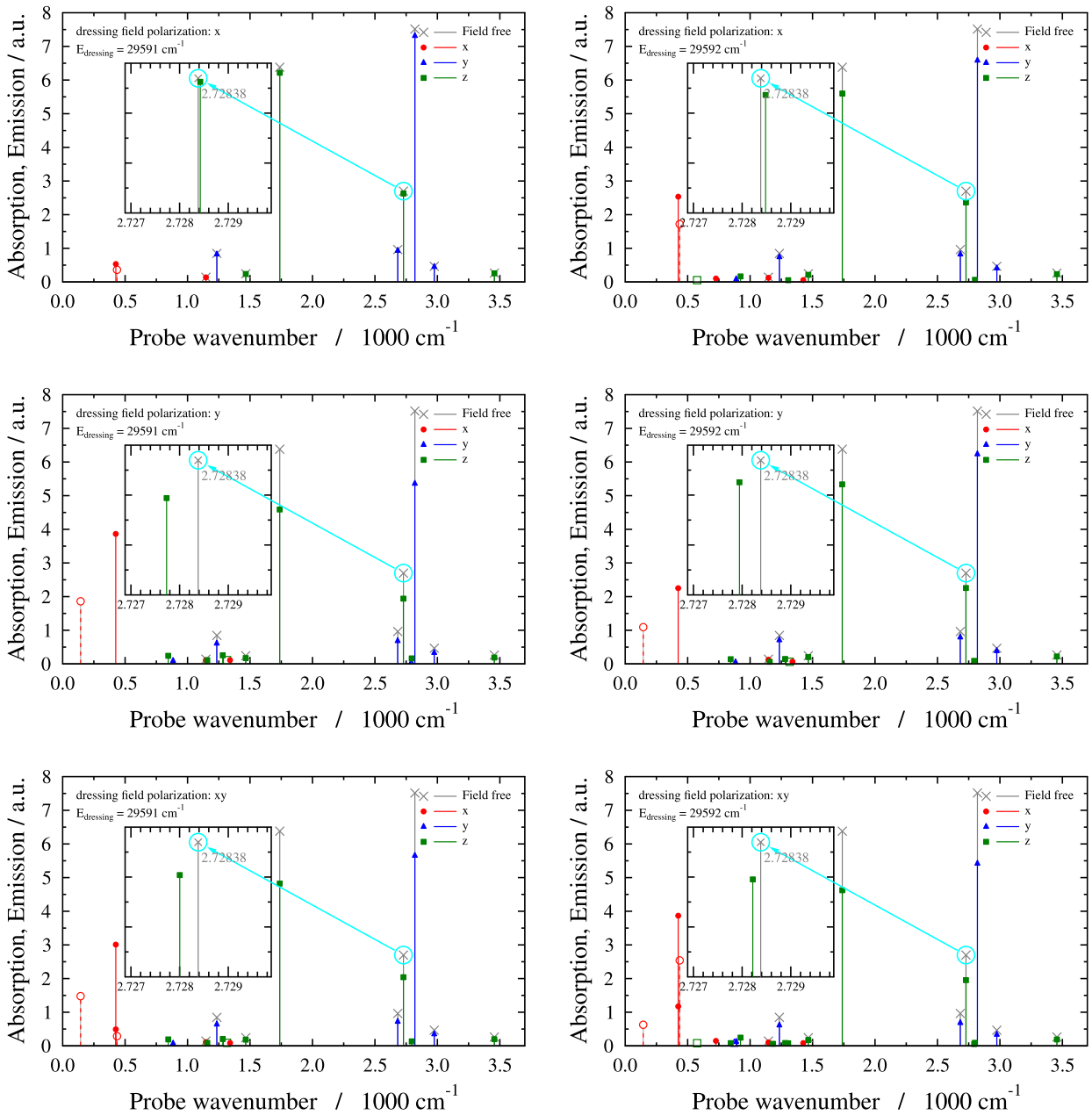

FIG. 5. Field-dressed and field-free spectra of the H_2CO molecule in the low-energy region. The dressing intensity equals $I_d = 10^{11}$ W/cm^2. The dressing wavenumber values (ω_d = 29 591.0 cm^{-1} and ω_d = 29 592.0 cm^{-1}) and polarization vectors [$\mathbf{e}_x$ = (1, 0, 0), $\mathbf{e}_y$ = (0, 1, 0), and $\mathbf{e}_{xy} = (1, 1, 0)/\sqrt{2}$] are given in the figure. Field-dressed transitions (absorption: solid lines and full markers; emission: dashed lines and empty markers) polarized along the x, y, and z axes are shown by the markers ●, ▲, and ■, respectively, while field-free transitions are indicated by the marker ×. It is apparent that the field-dressed spectrum exhibits peaks that are missing from the field-free spectrum and peaks of the field-free spectrum appear with reduced intensities in the field-dressed spectrum. Note the sensitivity of the field-dressed spectra to the dressing parameters.

vibrational mode (normal coordinates other than Q_2 are set to zero). In Fig. 3, the dressing wavenumber is set to ω_d = 29 592.0 cm^{-1} and the excited-state potential curve is shifted down with the energy of the dressing photon. Consequently, $|X0\rangle$ becomes nearly resonant with the closely lying vibrational states $|A, \nu_3 + \nu_4\rangle$ and $|A, 2\nu_4 + \nu_6\rangle$. Figure 4 displays two-dimensional cuts of the light-induced adiabatic PESs along the ν_2 and ν_4 vibrational modes for ω_d = 29 592.0 cm^{-1}, $I_d = 10^{14}$ W/cm^2, and $\mathbf{e} = \mathbf{e}_y$. The

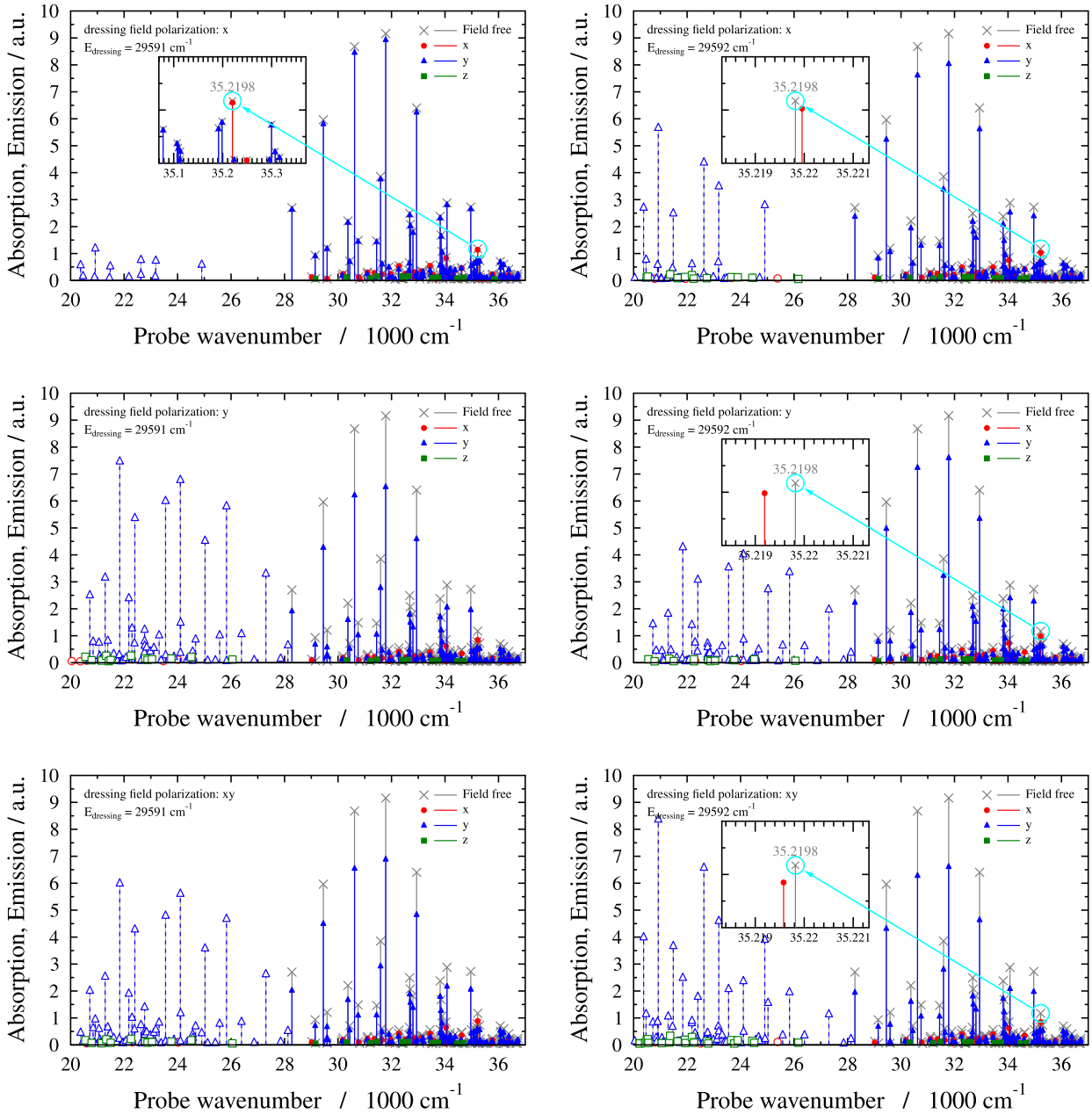

FIG. 6. Field-dressed and field-free spectra of the H_2CO molecule in the high-energy region. The dressing intensity equals $I_d = 10^{11}$ W/cm^2. The dressing wavenumber values (ω_d = 29 591.0 cm^{-1} and ω_d = 29 592.0 cm^{-1}) and polarization vectors [$\mathbf{e}_x$ = (1, 0, 0), $\mathbf{e}_y$ = (0, 1, 0), and $\mathbf{e}_{xy} = (1, 1, 0)/\sqrt{2}$] are given in the figure. Field-dressed transitions (absorption: solid lines and full markers; emission: dashed lines and empty markers) polarized along the *x*, *y*, and *z* axes are shown by the markers ●, ▲, and ■, respectively, while field-free transitions are indicated by the marker ×. It is apparent that the field-dressed spectrum exhibits peaks that are missing from the field-free spectrum and peaks of the field-free spectrum appear with reduced intensities in the field-dressed spectrum. Note the sensitivity of the field-dressed spectra to the dressing parameters.

two-dimensional cuts, given as functions of the Q_2 and Q_4 normal coordinates (the remaining four normal coordinates are set to zero), clearly show that a LICI is formed between the two light-induced adiabatic PESs. In what follows, the impact of the current dressing situation on the low-energy and high-energy regions of the field-dressed spectrum will be elucidated.

Figure 5 shows the field-free and field-dressed spectra of H_2CO in the low-energy region with ω_d = 29 591.0 cm^{-1} and

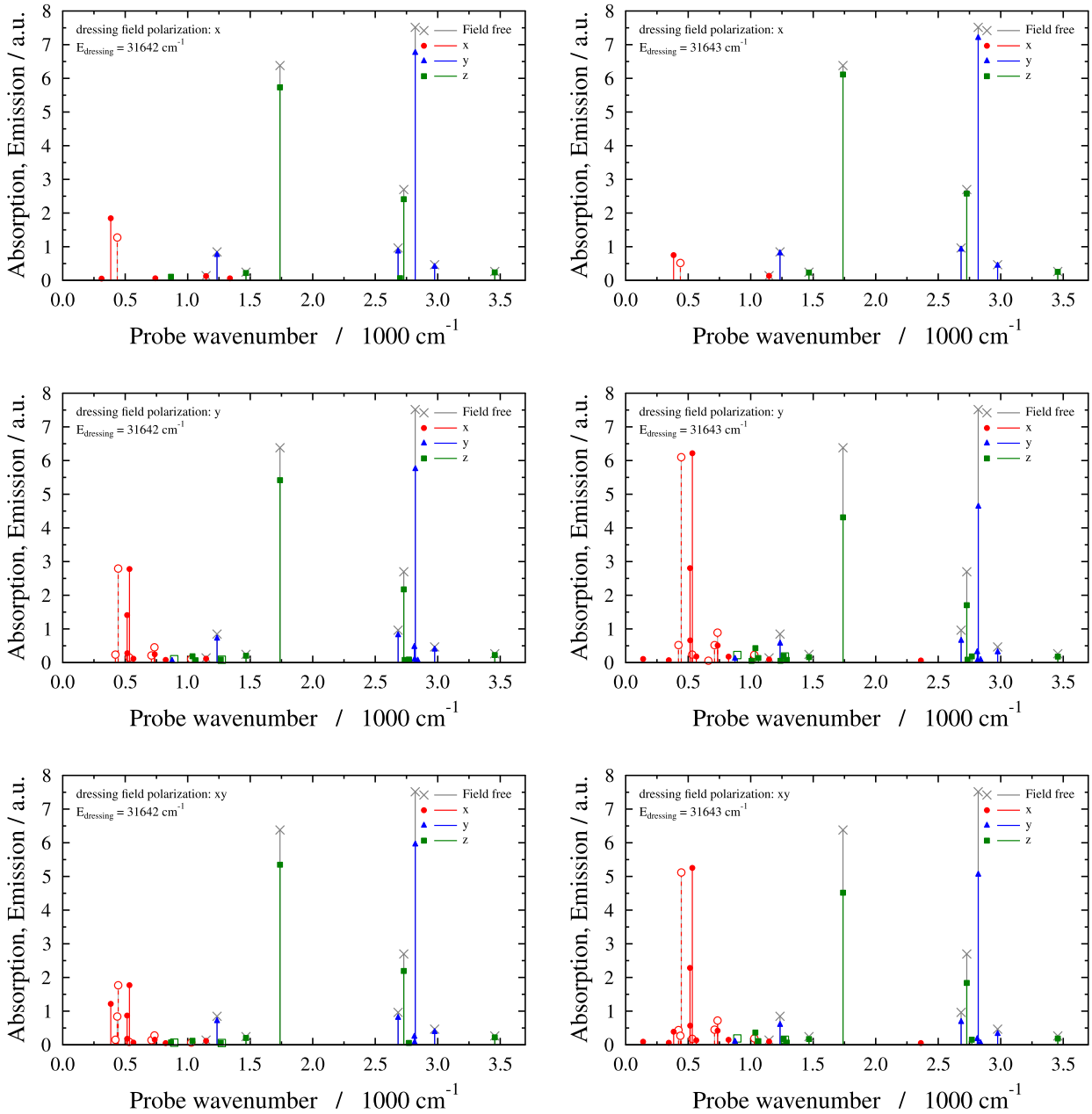

FIG. 7. Field-dressed and field-free spectra of the H_2CO molecule in the low-energy region. The dressing intensity equals $I_d = 10^{11}$ W/cm^2. The dressing wavenumber values (ω_d = 31 642.0 cm^{-1} and ω_d = 31 643.0 cm^{-1}) and polarization vectors [$\mathbf{e}_x$ = (1, 0, 0), $\mathbf{e}_y$ = (0, 1, 0), and $\mathbf{e}_{xy} = (1, 1, 0)/\sqrt{2}$] are given in the figure. Field-dressed transitions (absorption: solid lines and full markers; emission: dashed lines and empty markers) polarized along the *x*, *y*, and *z* axes are shown by the markers ●, ▲, and ■, respectively, while field-free transitions are indicated by the marker ×. It is apparent that the field-dressed spectrum exhibits peaks that are missing from the field-free spectrum and peaks of the field-free spectrum appear with reduced intensities in the field-dressed spectrum. Note the sensitivity of the field-dressed spectra to the dressing parameters.

ω_d = 29 592.0 cm^{-1}. For both values of ω_d, the dressing intensity was set to $I_d = 10^{11}$ W/cm^2 and the polarization vectors $\mathbf{e}_x$, $\mathbf{e}_y$, and $\mathbf{e}_{xy}$ were considered. The two ω_d values applied are in near resonance with the transitions $|X0\rangle$ (0.0 cm^{-1}, A_1) → $|A, \nu_3 + \nu_4\rangle$ (29 589.9 cm^{-1}, B_1) and $|X0\rangle$ (0.0 cm^{-1}, A_1) → $|A, 2\nu_4 + \nu_6\rangle$ (29 592.6 cm^{-1}, B_2), which induces mixing of $|X0\rangle$ with $|A, \nu_3 + \nu_4\rangle$ and $|A, 2\nu_4 + \nu_6\rangle$. As a result, the initial field-dressed state can be described as superposition of the states $|X0\rangle$, $|A, \nu_3 + \nu_4\rangle$, and

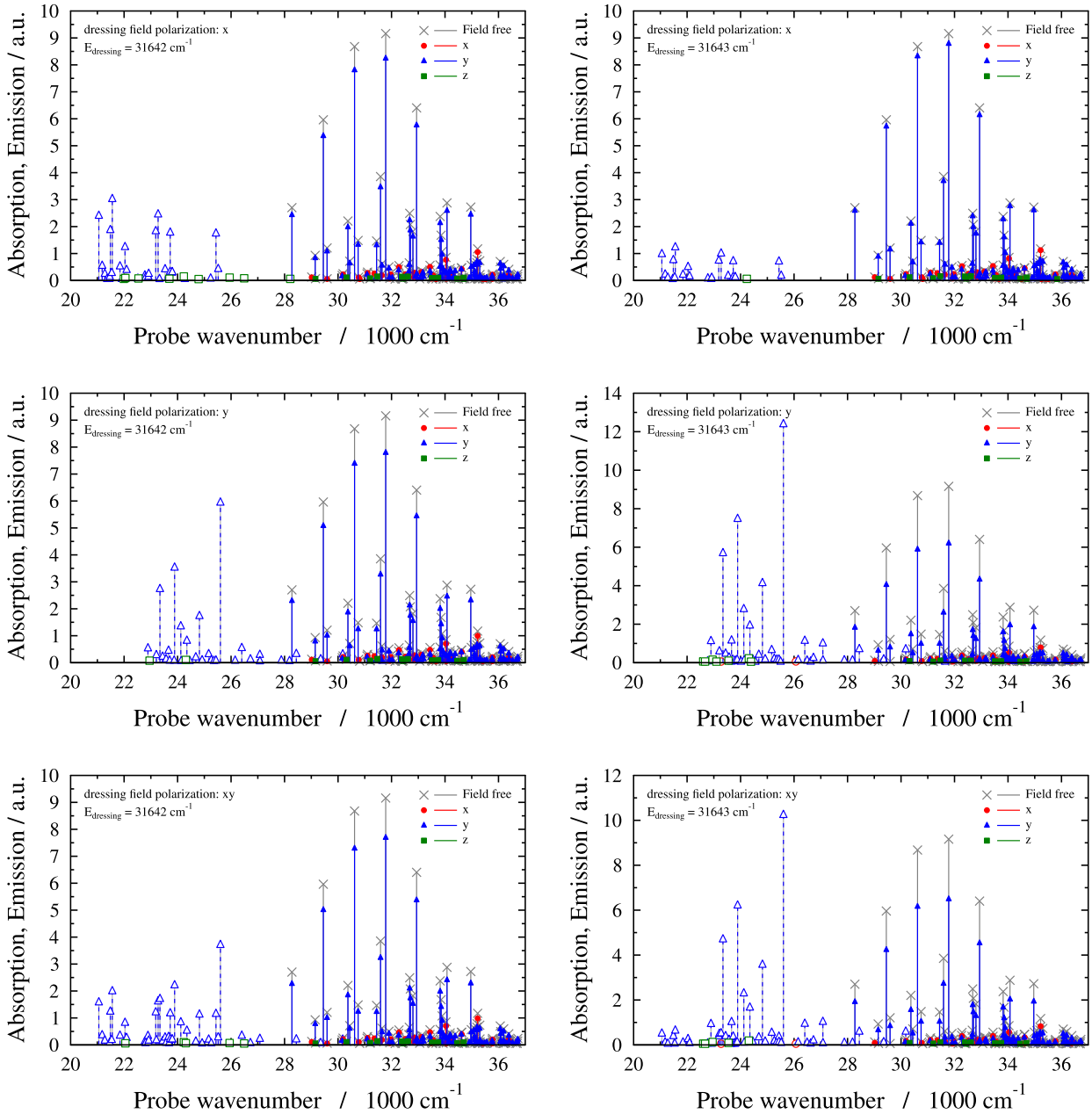

FIG. 8. Field-dressed and field-free spectra of the H_2CO molecule in the high-energy region. The dressing intensity equals $I_d = 10^{11}$ W/cm^2. The dressing wavenumber values (ω_d = 31 642.0 cm^{-1} and ω_d = 31 643.0 cm^{-1}) and polarization vectors [$\mathbf{e}_x$ = (1, 0, 0), $\mathbf{e}_y$ = (0, 1, 0), and $\mathbf{e}_{xy} = (1, 1, 0)/\sqrt{2}$] are given in the figure. Field-dressed transitions (absorption: solid lines and full markers; emission: dashed lines and empty markers) polarized along the *x*, *y*, and *z* axes are shown by the markers ●, ▲, and ■, respectively, while field-free transitions are indicated by the marker ×. It is apparent that the field-dressed spectrum exhibits peaks that are missing from the field-free spectrum and peaks of the field-free spectrum appear with reduced intensities in the field-dressed spectrum. Note the sensitivity of the field-dressed spectra to the dressing parameters.

$|\mathrm{A}, 2\nu_4 + \nu_6\rangle$, having the form of $|\Phi_i(n)\rangle$ in Eq. (15). An important prerequisite of this mixing process is that the energy of the dressing photon exceeds the X → A adiabatic excitation energy. Note that this criterion is not met in Sec. III A; therefore, no mixing of $|\mathrm{X0}\rangle$ with A vibrational states is possible in the dressing situation of Sec. III A.

The analysis of the numerical results has revealed that the final field-dressed states relevant for the low-energy region can be described as

$$|\Phi_f(n)\rangle = |\mathrm{X}f\rangle|n\rangle \tag{16}$$

and

$$|\Phi_{f'}(n)\rangle = |\mathrm{A}f'\rangle|n-1\rangle, \tag{17}$$

which gives rise to the transition amplitudes

$$\langle\Phi_i(n)|\hat{\mu}_\alpha|\Phi_f(n)\rangle = c^{(i)*}_{\mathrm{X}0n}\langle\mathrm{X0}|\hat{\mu}_\alpha|\mathrm{X}f\rangle \tag{18}$$

and

$$\langle\Phi_i(n)|\hat{\mu}_\alpha|\Phi_{f'}(n)\rangle = \sum_{\beta=1}^{m} c^{(i)*}_{\mathrm{A}k_\beta,n-1}\langle\mathrm{A}k_\beta|\hat{\mu}_\alpha|\mathrm{A}f'\rangle. \tag{19}$$

According to Eq. (18), peaks corresponding to the field-free transitions $|\mathrm{X0}\rangle \rightarrow |\mathrm{X}j\rangle$ will appear with reduced intensities in the low-energy field-dressed spectrum since $|c^{(i)*}_{\mathrm{X}0n}|^2 \leq 1$. The insets of Fig. 5 highlight a selected low-energy peak whose position and intensity are altered to different extents depending on the dressing field parameters. Equation (19) pertains to peaks that are missing from the field-free spectrum, but they are clearly visible in the low-energy field-dressed spectra of Fig. 5. These transitions (absorption or emission, depending on the energy of $|\Phi_{f'}(n)\rangle$) are associated with the PDM of the A electronic state, and their appearance in the field-dressed spectrum can be attributed to intensity borrowing from peaks of Eq. (18). It is apparent in Fig. 5 that the field-dressed spectra are highly sensitive to both the dressing wavenumber and the polarization vector of the dressing field. This effect originates in the dependence of $|\Phi_i(n)\rangle$ on the dressing parameters ω_d and $\mathbf{e}$. Due to symmetry, the state pairs $|\mathrm{X0}\rangle$ and $|\mathrm{A}, \nu_3 + \nu_4\rangle$, and $|\mathrm{X0}\rangle$ and $|\mathrm{A}, 2\nu_4 + \nu_6\rangle$ are coupled by the y and x components of the TDM, respectively. Therefore, changes in the direction of $\mathbf{e}$ tune the effective coupling matrix elements between the two state pairs mentioned, while the value of ω_d influences the energetic position of $|\mathrm{A}, \nu_3 + \nu_4\rangle$ and $|\mathrm{A}, 2\nu_4 + \nu_6\rangle$ relative to $|\mathrm{X0}\rangle$, as shown in Fig. 3. Clearly, both factors influence the composition of $|\Phi_i(n)\rangle$ and thus the peak structure of the field-dressed spectrum.

Figure 6 shows the field-free and field-dressed spectra of H_2CO in the high-energy region with the same dressing parameters as in Fig. 5. If we assume that the final field-dressed states relevant for the high-energy region take the form

$$|\Phi_f(n+1)\rangle = |\mathrm{A}f\rangle|n\rangle \tag{20}$$

and

$$|\Phi_{f'}(n-1)\rangle = |\mathrm{X}f'\rangle|n-1\rangle, \tag{21}$$

we get the transition amplitudes

$$\langle\Phi_i(n)|\hat{\mu}_\alpha|\Phi_f(n+1)\rangle = c^{(i)*}_{\mathrm{X}0n}\langle\mathrm{X0}|\hat{\mu}_\alpha|\mathrm{A}f\rangle \tag{22}$$

and

$$\langle\Phi_i(n)|\hat{\mu}_\alpha|\Phi_{f'}(n-1)\rangle = \sum_{\beta=1}^{m} c^{(i)*}_{\mathrm{A}k_\beta,n-1}\langle\mathrm{A}k_\beta|\hat{\mu}_\alpha|\mathrm{X}f'\rangle. \tag{23}$$

Equation (22) refers to transitions that correspond to absorption peaks in the field-dressed spectrum. These transitions appear in the upper half of the high-energy field-dressed spectrum, and their intensities are reduced compared to their field-free counterparts, which is readily explained by Eq. (22). A selected peak of this kind is displayed in the insets of Fig. 6 showing field-dependent changes in the position and intensity. Equation (23) characterizes field-dressed emission peaks that are missing from the field-free spectrum. The emission peaks are visible mainly in the lower half of the high-energy field-dressed spectrum, and they borrow intensity from the absorption peaks of Eq. (22). Similarly to the previous case, one can again notice the sensitivity of the field-dressed spectrum to ω_d and $\mathbf{e}$ due to the dependence of $|\Phi_i(n)\rangle$ on the dressing field parameters.

Figures 7 and 8 present the low-energy and high-energy field-free and field-dressed spectra of H_2CO with $\omega_\mathrm{d} = 31\,642.0\ \mathrm{cm}^{-1}$ and $\omega_\mathrm{d} = 31\,643.0\ \mathrm{cm}^{-1}$, $I_\mathrm{d} = 10^{11}\ \mathrm{W/cm}^2$, and the polarization vectors $\mathbf{e}_x$, $\mathbf{e}_y$, and $\mathbf{e}_{xy}$. As the current dressing wavenumbers are higher than the previously used values of $\omega_\mathrm{d} = 29\,591.0\ \mathrm{cm}^{-1}$ and $\omega_\mathrm{d} = 29\,592.0\ \mathrm{cm}^{-1}$, the higher-lying vibrational states $|\mathrm{A}, 2\nu_4 + \nu_5\rangle$ ($31\,640.7\ \mathrm{cm}^{-1}$, B_2) and $|\mathrm{A}, 2\nu_2 + 3\nu_4\rangle$ ($31\,643.7\ \mathrm{cm}^{-1}$, B_1) are mixed with $|\mathrm{X0}\rangle$ ($0.0\ \mathrm{cm}^{-1}$, A_1) by the dressing field. The field-dressed spectra in Figs. 7 and 8 show effects similar to the previously analyzed case, which can again be interpreted using the theoretical considerations of this subsection. What makes the field-dressed spectra in Figs. 7 and 8 different from the spectra in Figs. 5 and 6 is that $|\Phi_i(n)\rangle$ is now composed of $|\mathrm{X0}\rangle$, $|\mathrm{A}, 2\nu_4 + \nu_5\rangle$, and $|\mathrm{A}, 2\nu_2 + 3\nu_4\rangle$. Since these A vibrational states are different from $|\mathrm{A}, \nu_3 + \nu_4\rangle$ and $|\mathrm{A}, 2\nu_4 + \nu_6\rangle$ (which are relevant for the previous case with $\omega_\mathrm{d} = 29\,591.0\ \mathrm{cm}^{-1}$ and $\omega_\mathrm{d} = 29\,592.0\ \mathrm{cm}^{-1}$), the peak structures are noticeably altered compared to the previous case, primarily through the transition amplitude formulae in Eqs. (19) and (23).

IV. CONCLUSIONS

In the present work, fingerprints of light-induced nonadiabaticity have been investigated in the field-dressed spectrum of the formaldehyde (H_2CO) molecule. Both the low-energy and high-energy regions of the field-dressed spectrum have been carefully analyzed and compared to the field-free results by performing accurate full-dimensional quantum-dynamical calculations. We have also discussed in detail how the different laser frequencies and field polarization directions influence the impact of the LICI on the field-dressed spectrum. Our results clearly demonstrate that small changes in the parameters of the dressing field cause substantial changes in the field-dressed states and field-dressed spectra. We expect that dressing intensities higher than the value used in the

present work ($I_d = 10^{11}$ W/cm^2) will further enhance light-induced nonadiabatic effects.

For a lower dressing wavenumber ($\omega_d = 25\,575.0$ cm^{-1}), the low-energy part of the field-dressed spectrum practically remains unchanged. Neither new peaks nor splittings of peaks appear in this part of the field-dressed spectrum. This picture changes slightly if the high-energy part of the field-dressed spectrum is considered. Here, one can observe splittings of certain peaks of the field-free spectrum and it is also apparent from our results that the field-dressed spectrum is sensitive to both the dressing wavenumber and the polarization direction of the dressing field.

Turning to larger dressing wavenumbers (e.g., $\omega_d = 29\,592.0$ cm^{-1} or $\omega_d = 31\,642.0$ cm^{-1}), the situation changes dramatically and light-induced nonadiabaticity has a prominent signature on the field-dressed spectra. In addition to the appearance of emission peaks in the high-energy part of the field-dressed spectrum, one can also recognize the so-called intensity borrowing effect, which can be interpreted as a characteristic fingerprint of nonadiabatic phenomena, manifested by irregular variations of spectral peak intensities and the appearance of new energy levels.

ACKNOWLEDGMENTS

Professor Joel Bowman is gratefully acknowledged for providing Fortran subroutines for the S_0 and S_1 potential energy surfaces. We are indebted to Benjamin Lasorne for fruitful discussions. This research was supported by the EU-funded Hungarian Grant (No. EFOP-3.6.2-16-2017-00005). The authors acknowledge financial support from NKFIH (Grant No. K128396).

DATA AVAILABILITY

The data that support the findings of this study are available from the corresponding author upon reasonable request.

REFERENCES

[1] H. Köppel, W. Domcke, and L. S. Cederbaum, Adv. Chem. Phys. **57**, 59 (1984).
[2] D. R. Yarkony, Rev. Mod. Phys. **68**, 985 (1996).
[3] M. Baer, Phys. Rep. **358**, 75 (2002).
[4] G. A. Worth and L. S. Cederbaum, Annu. Rev. Phys. Chem. **55**, 127 (2004).
[5] W. Domcke, D. R. Yarkony, and H. Köppel, *Conical Intersections* (World Scientific, 2004).
[6] M. Baer, *Beyond Born–Oppenheimer: Electronic Non-Adiabatic Coupling Terms and Conical Intersections* (Wiley, New York, 2006).
[7] J. S. Lim and S. K. Kim, Nat. Chem. **2**, 627 (2010).
[8] D. Polli, P. Altoè, O. Weingart, K. M. Spillane, C. Manzoni, D. Brida, G. Tomasello, G. Orlandi, P. Kukura, R. A. Mathies, M. Garavelli, and G. Cerullo, Nature **467**, 440 (2010).
[9] H. J. Wörner, J. B. Bertrand, B. Fabre, J. Higuet, H. Ruf, A. Dubrouil, S. Patchkovskii, M. Spanner, Y. Mairesse, V. Blanchet, E. Mével, E. Constant, P. B. Corkum, and D. M. Villeneuve, Science **334**, 208 (2011).
[10] H. S. You, S. Han, J. S. Lim, and S. K. Kim, J. Phys. Chem. Lett. **6**, 3202 (2015).
[11] A. J. Musser, M. Liebel, C. Schnedermann, T. Wende, T. B. Kehoe, A. Rao, and P. Kukura, Nat. Phys. **11**, 352 (2015).
[12] A. von Conta, A. Tehlar, A. Schletter, Y. Arasaki, K. Takatsuka, and H. J. Wörner, Nat. Commun. **9**, 3162 (2018).
[13] M. E. Corrales, J. González-Vázquez, R. de Nalda, and L. Bañares, J. Phys. Chem. Lett. **10**, 138 (2019).
[14] P. Celani, F. Bernardi, M. Olivucci, and M. A. Robb, J. Am. Chem. Soc. **119**, 10815 (1997).
[15] G. Groenhof, M. Bouxin-Cademartory, B. Hess, S. P. de Visser, H. J. C. Berendsen, M. Olivucci, A. E. Mark, and M. A. Robb, J. Am. Chem. Soc. **126**, 4228 (2004).
[16] M. Boggio-Pasqua, M. J. Bearpark, F. Ogliaro, and M. A. Robb, J. Am. Chem. Soc. **128**, 10533 (2006).
[17] M. N. R. Ashfold, A. L. Devine, R. N. Dixon, G. A. King, M. G. D. Nix, and T. A. A. Oliver, Proc. Natl. Acad. Sci. U. S. A. **105**, 12701 (2008).
[18] T. J. Martinez, Nature **467**, 412 (2010).
[19] X. Xu, J. Zheng, K. R. Yang, and D. G. Truhlar, J. Am. Chem. Soc. **136**, 16378 (2014).
[20] M. Kowalewski, K. Bennett, K. E. Dorfman, and S. Mukamel, Phys. Rev. Lett. **115**, 193003 (2015).
[21] C. Xie, J. Ma, X. Zhu, D. R. Yarkony, D. Xie, and H. Guo, J. Am. Chem. Soc. **138**, 7828 (2016).
[22] J. A. DeVine, M. L. Weichman, X. Zhou, J. Ma, B. Jiang, H. Guo, and D. M. Neumark, J. Am. Chem. Soc. **138**, 16417 (2016).
[23] K. C. Woo, D. H. Kang, and S. K. Kim, J. Am. Chem. Soc. **139**, 17152 (2017).
[24] B. F. E. Curchod and T. J. Martínez, Chem. Rev. **118**, 3305 (2018).
[25] N. Ismail, L. Blancafort, M. Olivucci, B. Kohler, and M. A. Robb, J. Am. Chem. Soc. **124**, 6818 (2002).
[26] J. D. Coe and T. J. Martínez, J. Am. Chem. Soc. **127**, 4560 (2005).
[27] M. Boggio-Pasqua, G. Groenhof, L. V. Schäfer, H. Grubmüller, and M. A. Robb, J. Am. Chem. Soc. **129**, 10996 (2007).
[28] A. Migani, M. J. Bearpark, M. Olivucci, and M. A. Robb, J. Am. Chem. Soc. **129**, 3703 (2007).
[29] M. Boggio-Pasqua, M. A. Robb, and G. Groenhof, J. Am. Chem. Soc. **131**, 13580 (2009).
[30] S. Matsika and D. R. Yarkony, J. Am. Chem. Soc. **125**, 12428 (2003).
[31] C. Xie, C. L. Malbon, D. R. Yarkony, D. Xie, and H. Guo, J. Am. Chem. Soc. **140**, 1986 (2018).
[32] N. Moiseyev, M. Šindelka, and L. S. Cederbaum, J. Phys. B: At., Mol. Opt. Phys. **41**, 221001 (2008).
[33] M. Šindelka, N. Moiseyev, and L. S. Cederbaum, J. Phys. B: At., Mol. Opt. Phys. **44**, 045603 (2011).
[34] G. J. Halász, Á. Vibók, M. Šindelka, N. Moiseyev, and L. S. Cederbaum, J. Phys. B: At., Mol. Opt. Phys. **44**, 175102 (2011).
[35] G. J. Halász, M. Šindelka, N. Moiseyev, L. S. Cederbaum, and Á. Vibók, J. Phys. Chem. A **116**, 2636 (2011).
[36] G. J. Halász, A. Vibók, N. Moiseyev, and L. S. Cederbaum, Phys. Rev. A **88**, 043413 (2013).
[37] G. J. Halász, P. Badankó, and Á. Vibók, Mol. Phys. **116**, 2652 (2018).
[38] A. Natan, M. R. Ware, V. S. Prabhudesai, U. Lev, B. D. Bruner, O. Heber, and P. H. Bucksbaum, Phys. Rev. Lett. **116**, 143004 (2016).
[39] G. J. Halász, Á. Vibók, and L. S. Cederbaum, J. Phys. Chem. Lett. **6**, 348 (2015).
[40] A. Csehi, G. J. Halász, L. S. Cederbaum, and Á. Vibók, Faraday Discuss. **194**, 479 (2016).
[41] A. Csehi, G. J. Halász, L. S. Cederbaum, and Á. Vibók, Phys. Chem. Chem. Phys. **19**, 19656 (2017).
[42] A. Csehi, G. J. Halász, L. S. Cederbaum, and A. Vibók, *Attosecond Molecular Dynamics* (The Royal Society of Chemistry, 2018), pp. 183–217.
[43] T. Szidarovszky, G. J. Halász, A. G. Császár, L. S. Cederbaum, and Á. Vibók, J. Phys. Chem. Lett. **9**, 2739 (2018).
[44] J. Kim, H. Tao, J. L. White, V. S. Petrović, T. J. Martinez, and P. H. Bucksbaum, J. Phys. Chem. A **116**, 2758 (2012).
[45] M. E. Corrales, J. González-Vázquez, G. Balerdi, I. R. Solá, R. de Nalda, and L. Bañares, Nat. Chem. **6**, 785 (2014).
[46] P. V. Demekhin and L. S. Cederbaum, J. Chem. Phys. **139**, 154314 (2013).
[47] C. Fábri, B. Lasorne, G. J. Halász, L. S. Cederbaum, and Á. Vibók, J. Phys. Chem. Lett. **11**, 5324 (2020).
[48] M. Araujo, B. Lasorne, M. J. Bearpark, and M. A. Robb, J. Phys. Chem. A **112**, 7489 (2008).

[49]M. Araújo, B. Lasorne, A. L. Magalhães, G. A. Worth, M. J. Bearpark, and M. A. Robb, J. Chem. Phys. **131**, 144301 (2009).
[50]M. Araújo, B. Lasorne, A. L. Magalhães, M. J. Bearpark, and M. A. Robb, J. Phys. Chem. A **114**, 12016 (2010).
[51]S.-I. Chu, J. Chem. Phys. **75**, 2215 (1981).
[52]S.-I. Chu and D. A. Telnov, Phys. Rep. **390**, 1 (2004).
[53]P. L. Knight and L. Allen, Phys. Rev. A **7**, 368 (1973).
[54]D. C. Clary, J. Phys. Chem. **87**, 735 (1983).
[55]M. A. Kmetic, R. A. Thuraisingham, and W. J. Meath, Phys. Rev. A **33**, 1688 (1986).
[56]T. Szidarovszky, A. G. Császár, G. J. Halász, and A. Vibók, Phys. Rev. A **100**, 033414 (2019).
[57]X. Wang, P. L. Houston, and J. M. Bowman, Philos. Trans. R. Soc., A **375**, 20160194 (2017).
[58]B. Fu, B. C. Shepler, and J. M. Bowman, J. Am. Chem. Soc. **133**, 7957 (2011).
[59]E. Mátyus, G. Czakó, and A. G. Császár, J. Chem. Phys. **130**, 134112 (2009).
[60]C. Fábri, E. Mátyus, and A. G. Császár, J. Chem. Phys. **134**, 074105 (2011).
[61]A. G. Császár, C. Fábri, T. Szidarovszky, E. Mátyus, T. Furtenbacher, and G. Czakó, Phys. Chem. Chem. Phys. **14**, 1085 (2012).
[62]X. Chapuisat and C. Iung, Phys. Rev. A **45**, 6217 (1992).
[63]C. Eckart, Phys. Rev. **47**, 552 (1935).
[64]P. Bunker and P. Jensen, *Molecular Symmetry and Spectroscopy* (NRC Research Press, 2006).
[65]E. Mátyus, G. Czakó, B. T. Sutcliffe, and A. G. Császár, J. Chem. Phys. **127**, 084102 (2007).
[66]C. Fábri, E. Mátyus, T. Furtenbacher, L. Nemes, B. Mihály, T. Zoltáni, and A. G. Császár, J. Chem. Phys. **135**, 094307 (2011).
[67]S. H. Autler and C. H. Townes, Phys. Rev. **100**, 703 (1955).